Protein Science (1997), 6:1849–1857. Cambridge University Press. Printed in the USA.

Backbone makes a significant contribution to the electrostatics of α/β-barrel proteins

SOUMYA RAYCHAUDHURI,[1] FAYYAZ YOUNAS,[2] P. ANDREW KARPLUS,[3] CARLOS H. FAERMAN,[3] AND DANIEL R. RIPOLL[4]

[1]Department of Biophysics, State University of New York at Buffalo, Buffalo, New York 14214
[2]Department of Computer Science, State University of New York at Stony Brook, Stony Brook, New York 11794
[3]Section of Biochemistry, Department of Molecular and Cell Biology, Cornell University, Ithaca, New York 14853
[4]Cornell Theory Center, Cornell University, Ithaca, New York 14853

(RECEIVED January 27, 1997; ACCEPTED May 15, 1997)

Abstract

The electrostatic properties of seven α/β-barrel enzymes selected from different evolutionary families were studied: triose phosphate isomerase, fructose-1,6-bisphosphate aldolase, pyruvate kinase, mandelate racemase, trimethylamine dehydrogenase, glycolate oxidase, and narbonin, a protein without any known enzymatic activity. The backbone of the α/β-barrel has a distinct electrostatic field pattern, which is dipolar along the barrel axis. When the side chains are included in the calculations the general effect is to modulate the electrostatic pattern so that the electrostatic field is generally enhanced and is focused into a specific area near the active site. We use the electrostatic flux through a square surface near the active site to gauge the functionally relevant magnitude of the electrostatic field. The calculations reveal that in six out of the seven cases the backbone itself contributes greater than 45% of the total flux. The substantial electrostatic contribution of the backbone correlates with the known preference of α/β-barrel enzymes for negatively charged substrates.

Keywords: α/β-barrel; electrostatic flux and field; enzymes; substrate charge

The α/β-barrel structure, first observed in triose phosphate isomerase (TIM), has now been found in approximately 10% of all enzymes with known structures (Banner et al., 1975; Reardon & Farber, 1995). A wide variety of enzymes catalyzing very different types of reactions exhibit this fold and for this reason it has been designated as a superfold (Orengo et al., 1994). The α/β-barrel structure, illustrated in Figure 1, consists of a series of eight parallel β-sheets arranged in a barrel formation surrounded by α-helices, which connect the parallel strands of the β-sheets and run antiparallel to the β-sheets, in such a manner that the N-terminus of each α-helix is adjacent to the C-terminal ends of the two neighboring strands of the β-sheet. The cross-section of the barrel is usually elliptical. The loops between the β-sheets and the α-helices can be of variable length and may adopt various conformations. Despite these differences, arguments have been made in favor of divergent evolution of the α/β-barrel proteins from a common ancestor (Farber, 1993; Baldwin et al., 1995).

Although most of the proteins that contain the α/β-barrel fold account for a wide variety of enzymatic activities, the active site is consistently situated at the C-terminal end of the β-barrel (Farber & Petsko, 1990). Hol et al. (1978) proposed that the amino end of a suitably positioned α-helix provides a local electrostatic dipole moment, which could explain the location of the binding crevices at the C-terminal end of the β-strands. Bränden (1980) suggested that the α/β-barrels are also topologically favorable for forming binding crevices at the C-terminal end of the β-strands, and most crevices are used for binding negatively charged substrates. It is unknown whether the observed preference of α/β-barrel enzymes for negatively charged substrates is a unique phenomenon of this fold or simply a result of the high occurrence of negatively charged metabolites.

Studies of the electrostatic properties of complex biological molecules, relying on continuum models, have allowed investigators to develop quantitative descriptions of electrostatic potentials, diffusion-limited processes, pH-dependent properties, ionic-strength phenomena, and solvation free energies (Honig & Nicholls, 1995). In particular, studies of the electrostatic properties of several enzymes utilizing such methods have led to functional insights. For instance, the very high activity of superoxide dismutase (SOD) is partly due to electrostatic steering. Overall, its electrostatic isopotential surface is negative but, near the active site, SOD has a small area where the isopotential is positive that attracts the negatively charged superoxide substrate (Klapper et al., 1986; Getzoff et al., 1992). Similarly, in acetylcholinesterase, the protein generates an electrostatic field that plays a critical role in guiding its positively charged substrate, acetylcholine, towards the active site (Ripoll

Reprint requests to: Daniel R. Ripoll, Cornell Theory Center, Cornell University, 535 Frank Rhodes Building, Ithaca, New York 14853; e-mail: ripoll@tc.cornell.edu.

Fig. 1. The prototypic $(\alpha/\beta)_8$-barrel domain of TIM is viewed from the C-terminal end, which we define as the top of the barrel. This plot was obtained with the program MOLSCRIPT (Kraulis, 1991). The C-terminus of the β-strands is pointing mainly towards the reader. We rotated the α/β-barrel to the left so that this orientation is as close as possible to the one shown in Fig. 2M.

et al., 1993; Gilson et al., 1994). TIM has been extensively studied and it has been shown that the enzyme's electrostatic field can help steer the negatively charged substrate glyceraldehyde 3-phosphate into its active site (Luty et al., 1993). Also, electrostatic properties of proteins have been suggested to stabilize mixed α/β folds more than pure α-helical or β-strand structures (Spassov et al., 1994). Recently, Schreiber et al. (1996) showed that the rapid association of barnase and its intracellular inhibitor barstar is dominated by long-range electrostatic forces.

In an effort to provide additional insight to our current understanding of α/β-barrel enzymes and their frequent occurrence, we focus our attention on the electrostatic properties of this protein family. We address two important interrelated questions: Whether there is any similarity among the electrostatic properties of the different α/β-barrel proteins that can account for their preference for negatively charged substrates, and what the contribution of the backbone is to the overall electrostatics of the α/β-barrel. We use the concept of electrostatic flux to compare the relative contribution of the backbone and the side chains to the electrostatic properties of enzymes that exhibit the α/β-barrel fold. Based on our results we conclude that the backbone contributes substantially to the distinct global electrostatic pattern of α/β-barrel proteins, which helps explain the marked preference for negatively charged substrates.

Results and discussion

Rationale for electrostatic flux

The comparison of the electrostatic properties of two different charge distributions, for example due to the backbone versus the full protein, is a complicated task. The simplest method is to compare the net charge of the molecules. In general, the net charge is not a very telling parameter to characterize the electrostatic properties of enzymes. For example, the net charge of the seven α/β-barrel enzymes studied here range from $-12.0e$ to $+3.0e$. There is, however, little or no correlation between net charge of these enzymes and the charge of their substrates (or inhibitors).

A second alternative is to use the electrostatic potential. This scalar magnitude is probably the most commonly used to describe the electrostatic properties of molecules (Nakamura, 1996). Typically, it can be displayed as isopotential surfaces or mapped onto a given surface (e.g., the molecular surface). The major drawback of using isopotential surfaces for a comparison of charge distributions is that an isopotential itself yields no insight into the electrostatic force acting upon a charged substrate or inhibitor. For that, one needs at least two isopotential surfaces for each distribution because the electrostatic force acting upon a charged substrate or inhibitor is proportional to the gradient of the electrostatic potential generated by an enzyme:

$$\vec{F}(\vec{r}) = q_{subs}\vec{E}(\vec{r}) = -q_{subs}\vec{\nabla}\Phi$$

where q_{subs} is the substrate charge, $\vec{F}(\vec{r})$ is the force, $\vec{E}(\vec{r})$ is the electrostatic field, and Φ is the potential.

On the other hand, the potential mapped onto the molecular surface or a plane is easier to interpret than the isopotential surfaces since the variations in color are directly related to the surface component of the gradient of the electrostatic potential. These two techniques that deal with electrostatic potentials provide complementary information on a single charge distribution but are difficult to use for comparing two distributions.

A third possibility is to compare directly the electrostatic fields generated by two charge distributions. Since $\vec{E}(\vec{r})$ is a vectorial quantity that depends on the specific position vector in space, $\vec{r}$, the comparison of two fields for every point of space is quite difficult to interpret.

We have found that a reasonable technique to *quantify* local differences between two different charge distributions is to compute the electrostatic flux through a given surface. Using the electrostatic flux, we have shown that a seven-residue mutant of human acetylcholinesterase, which shows a much-reduced isopotential surface, still exhibits a substantial electrostatic attraction for acetylcholine near the entrance to the active-site gorge (Ripoll et al., 1995), in agreement with the experimental observations and theoretical calculations based on Brownian dynamics (Antosiewicz et al, 1995). The results of our approach contrast with the inferences drawn by Shafferman et al. (1994) from viewing the reduction of a single isopotential surface: They concluded that electrostatics does not play an important role in human acetylcholinesterase.

Backbone versus side chain contribution to electrostatics

We examined the electrostatic properties of seven diverse α/β-barrel proteins (Reardon & Farber, 1995): TIM, fructose-1,6-bisphosphate aldolase, pyruvate kinase, mandelate racemase, trimethylamine dehydrogenase (TMADH), glycolate oxidase, and narbonin (NAR). Figure 1 shows the α/β-barrel of TIM viewed from the C-terminal end of the β-strands, which we define as the top of the barrel. The electrostatic fields generated by the enzymes are rather complex, although most of them have a "cylinder-like" shape. To assess the contribution of the backbone to the overall electrostatic properties of the α/β-barrel, we calculated the elec-

Table 1. *The electrostatic flux (kTÅ/e) in the vicinity of the active site*

Protein name	Backbone[a] (b)	Full[a] (f)	b/f Flux ratio[a] (%)	Net protein charge (*e*)	Net substrate charge (*e*)
1fba	1.0 (1.1)	2.2 (2.1)	45 (52)	−1.0	−3.0
1gyl	2.6 (2.4)	5.4 (5.2)	48 (46)	3.0	−1.0
1pkn	2.2 (2.4)	3.3 (3.2)	66 (75)	−1.0	−3.0
2mnr	1.7 (1.7)	3.4 (3.6)	50 (47)	−3.0	−1.0
2tmd	1.9 (1.4)	−13.1 (−12.4)	—[b]	−11.0	1.0
2tmd(no loop)[c]	2.0 (1.7)	3.7 (3.3)	54 (52)	−8.0	1.0
1nar	3.7 (3.4)	3.9 (3.5)	95 (97)	−12.0	Not known
1tim	2.3 (2.1)	3.1 (2.6)	74 (81)	0.0	−2.0

[a]All the flux results were computed using a grid of 65^3 points, whereas the values in parenthesis correspond to a grid of 129^3 points.
[b]Value not calculated because the flux changes sign.
[c]Calculation for TMADH where the residues contained in the loop G259–H278 were removed.

trostatic field for the backbone only and compared it with the full α/β-fold. The net charges for the backbone only are zero in all cases, whereas they vary from −12.0*e* to 3.0*e* (Table 1) for each enzyme.

Figure 2 shows the results of these calculations for a plane that cuts across the active site of each protein. The seven proteins analyzed have a similar electrostatic pattern due to the backbone. A negatively charged substrate would be guided into the enzyme's active site by a inward force, and in the absence of any other external forces[5] would follow a trajectory on the plane indicated by the yellow-to-blue lines (Fig. 2). Furthermore, the electrostatic potential due to the backbone, when projected onto the intersecting plane, is in each case positive (either dark or light blue). This shows clearly that the α/β-backbone contribution to the electrostatic field is quite similar in each case analyzed.

Adding the atomic charges of the side chains generally changes the electrostatic field pattern in such a way as to "enhance" the attraction into specific areas near the active site, as shown in Figure 2. The electrostatic field lines become denser as they get closer to the active site region. A magnitude that helps us quantify this effect is the variation in the electrostatic flux through a small surface. Two cases are analyzed: Partial charges only on the α/β-barrel backbone atoms, and partial charges on all atoms. In all calculations, the flux is computed on a square surface positioned near the active site. The position of this surface element is kept fixed in both sets of calculations (see Methods). As summarized in Table 1, the enhancement of the flux is well defined for fructose-1,6-bisphosphate aldolase, glycolate oxidase, and mandelate racemase, (enhancement of the flux ranges from 2.0 to 2.2), whereas for TIM, piruvate kinase, and narbonin the "focusing" is less pronounced (flux increases range from 1.1 to 1.3). The electrostatic flux clearly shows the substantial contribution of the backbone, and the enhancement due to the side chains, an effect needed to attract a negatively charged substrate into the catalytic site. The only exception is TMADH, an enzyme that binds a positively charged substrate, for which the electrostatic fields of the whole α/β-barrel and the backbone point in opposite directions.

Hol (1978) observed that the active site in many enzymes is located at the N-terminus of an α-helix, and thus proposed that the α-helix local electrostatic dipole moment plays an important role in substrate binding. We find that, in addition to local effects, for the α/β-barrel enzymes, all the α-helices together give rise to a global electrostatic effect that contributes to substrate binding.

[5]In the absence of an external field, a particle moves randomly between collisions with other particles. This motion is called Brownian motion.

Discussion of three specific cases

We will now concentrate on three specific cases: TIM as a general example of the electrostatic results obtained here, and TMADH and NAR as two additional enzymes that illustrate exceptional features.

Triose phosphate isomerase

TIM is an example that nicely summarizes the general features of our results: The α/β-barrel backbone gives rise to an electrostatic potential of dipolar character with the C-terminal end of the barrel embedded in a region of positive potential values. The associated electrostatic field should lead negatively charged molecules toward the active site, as indicated in Figure 2M, by the large number of electrostatic lines converging to the active site region. The electrostatic potential of the TIM backbone mapped onto the molecular surface is displayed in Figure 2O. This figure shows the active-site region surrounded by the most positive electrostatic potential values.

The electrostatic potential due to the whole molecule is more complex and different from that of the backbone alone. However, some of the features observed in the "backbone-only" calculation are maintained, e.g., the active site is still immersed in a region of highly positive potential values, as seen in Figure 2P. Furthermore, the electrostatic field, now due to the whole molecule, still remains directed toward the C-terminal end of the α/β-barrel as shown in Figure 2N. Our calculations also indicate that the backbone contribution to the flux near the active-site region is quite substantial, near 75% (Table 1).

There are two cases that deserve further examination: TMADH and narbonin. The former catalyzes a reaction involving a positively charged substrate whereas the latter has no known enzymatic activity.

Trimethylamine dehydrogenase

TMADH is an iron-sulfur flavoprotein found in several methyltrophic bacteria that catalyze the oxidative N-demethylamination of trimethylamine to form dimethylamine and formaldehyde (Lim

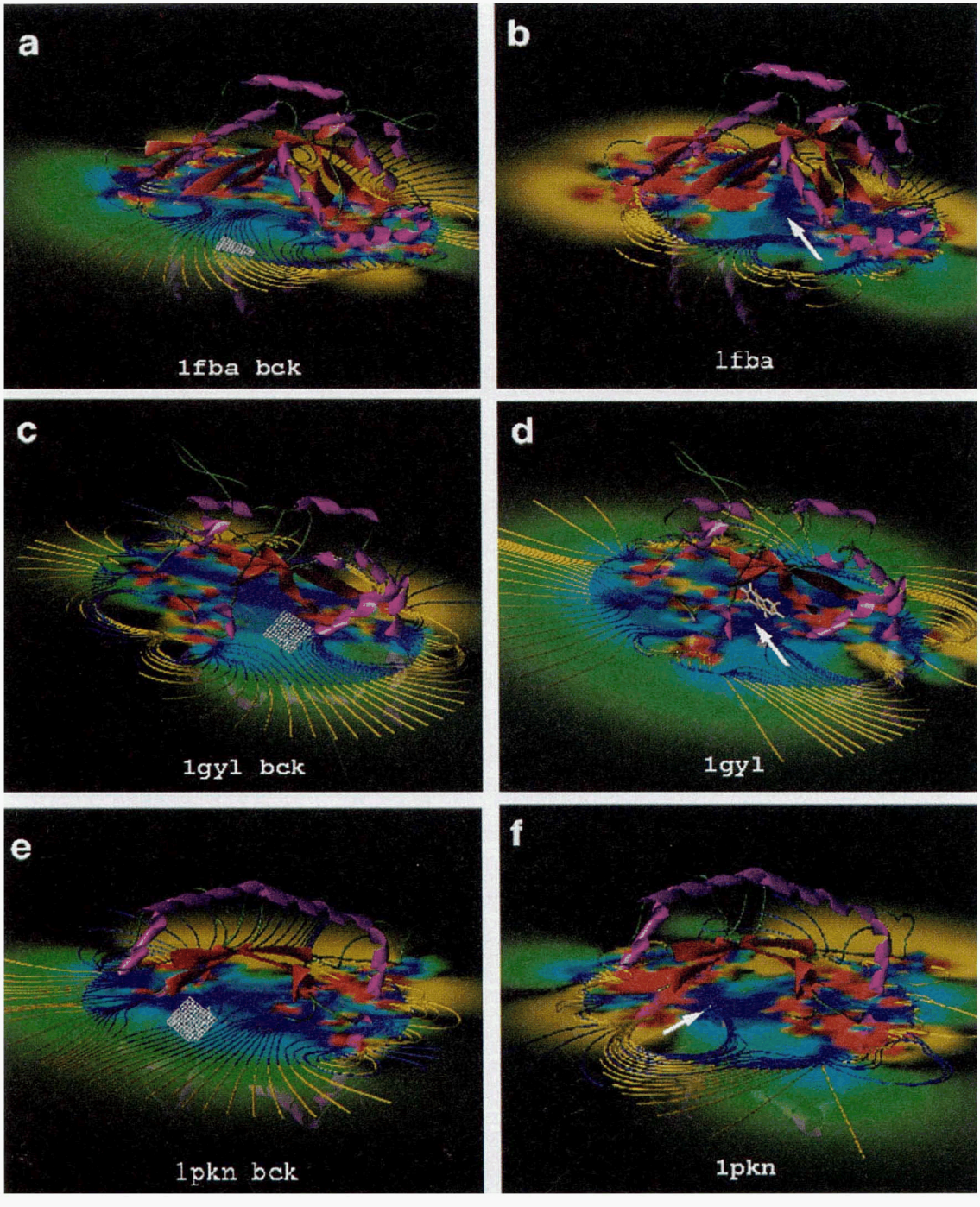

Fig. 2. The electrostatic properties of each of the seven α/β-barrel enzymes are shown for the backbone atoms only (left side panels) and for the entire α/β-barrel (right side panels). The following enzymes are displayed: **A–B:** fructose-1,6-bisphosphate aldolase (1fba); **C–D:** glycolate oxidase (1gyl); **E–F:** pyruvate kinase (1pkn); **G–H:** mandelate racemase (2mnr); **I–J:** trimethylamine dehydrogenase (2tmd); **K–L:** narbonin (1nar); **M–P:** triose phosphate isomerase (1tim). The four-character code that labels each panel is the Brookhaven Protein Data Bank entry code for the coordinate set (Bernstein et al., 1977). The ribbon representation of each enzyme is colored by secondary structure: α-helices are magenta, β-strands are red, and connecting segments are green. In all the cases, the orientation of the enzyme is similar to the one shown in Fig. 1. A plane that intersects the active site and contains the barrel axis is colored according to the values of the electrostatic potential: Dark blue, light blue, green, black, yellow, red represent decreasing values of the electrostatic potential. In addition to this, the electrostatic field lines are projected onto the intersecting plane. The direction of the field is such that a negatively charged substrate would experience a force from a yellow to a blue line. In panels A, C, E, G, I, K, and M, the position of the square grids used to calculate the electrostatic flux are shown. The white arrows, in panels B, D, F, H, J, and N, indicate the position of the active site regions for these enzymes. This figure was generated using the program Data Explorer™ IBM (A–N) and GRASP (O–P). (*Figure continues on following pages.*)

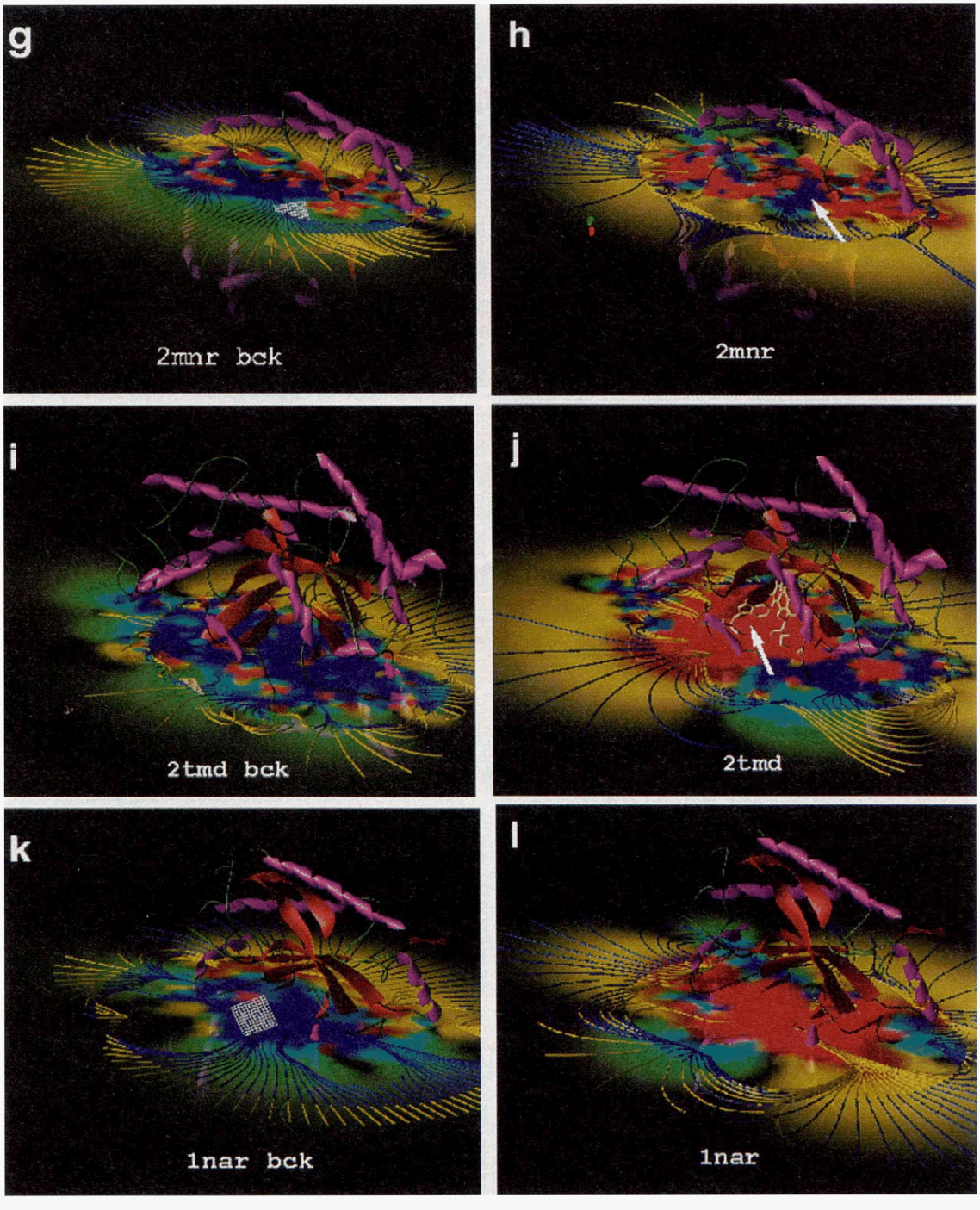

Fig. 2. *Continues.*

et al., 1986, 1988; Bellamy et al., 1989; Barber et al., 1992). The structure of the TMADH dimer is composed of six domains, described as the L1, L2 (large), M1, M2 (medium), and S1, S2 (small) domains following the nomenclature of Lim et al. (1986). Both L domains correspond to α/β-barrels. The active sites are located at the C-terminals of the L domains. They are, however, deeply buried within the enzyme, covered by S1 and S2 domains. The substrate appears to travel through long and negatively charged channels to get to the active-site centers.

To compare the electrostatic properties of the TMADH barrel with the other α/β-barrel proteins described above, we have studied an isolated α/β-barrel domain (L1) of TMADH (residues 1 to 382). Upon cursory inspection, the electrostatic pattern for TMADH (Fig. 2J) appears to be quite different from the other enzymes discussed thus far. Figure 2J shows the electrostatic potential and field for this α/β-barrel projected onto a plane. The values of the electrostatic flux for TMADH calculated for a 129^3 grid, 1.4 kTÅ/e for the backbone and -12.4 kTÅ/e for the whole α/β-barrel

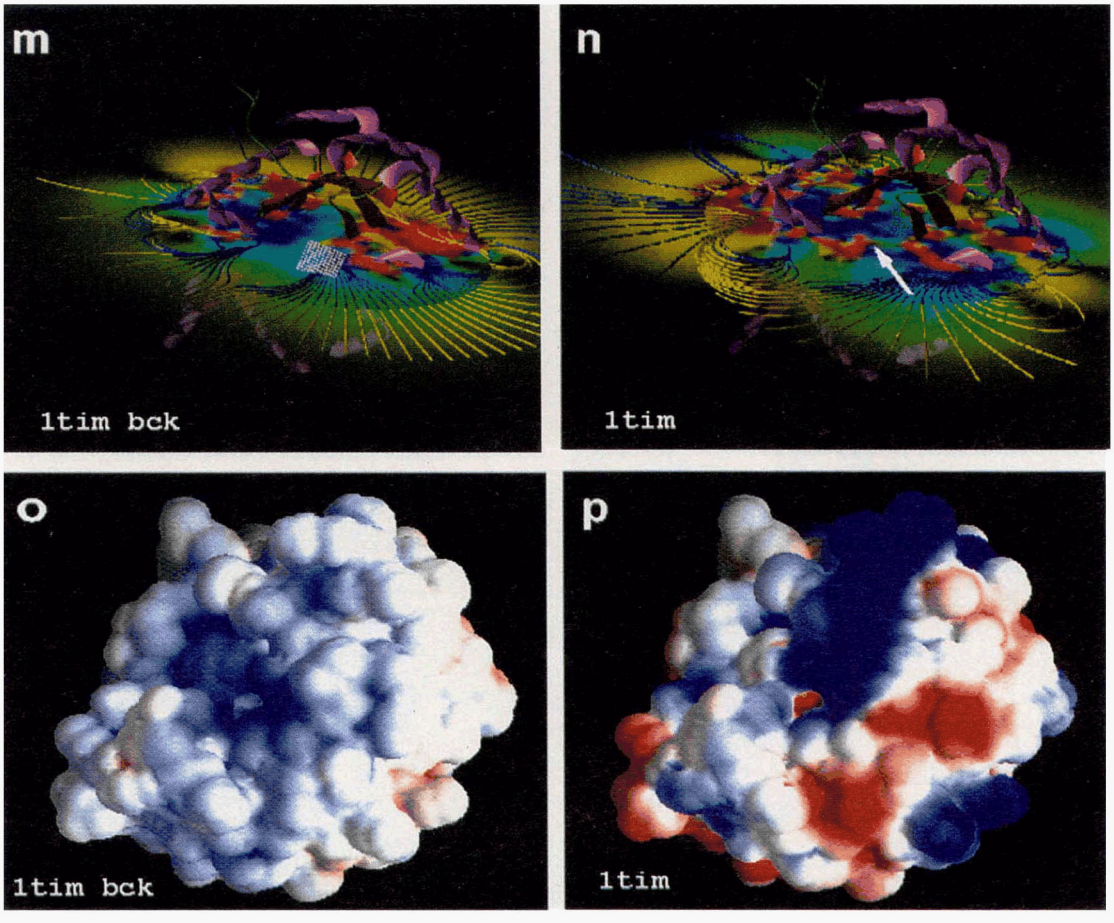

Fig. 2. *Continued.*

(Table 1) indicate that the electrostatic field due to the backbone is approximately opposite to the net electrostatic field due to the whole α/β-barrel. Examination of the C-terminal end of the isolated α/β-barrel domain indicates that highly positive and negative potential values coexist in this region. The positive patch at the C-terminal of the α/β-barrel (Fig. 2J, right-hand side) is very prominent and consistent with the backbone pattern found in the present work. This positive region includes the binding sites of the cofactor FMN, a negatively charged molecule due to its phosphoryl group, and the cofactor 4Fe–4S (iron/sulfur cluster), both of which are essential for catalysis.

The backbone contribution to the positive potential in this region is enhanced by adding the side chains of residues R299 and R322. The negative potential values (Fig. 2J, left-hand side) can be largely ascribed to four acidic residues D260, E263, E266, and D267 contained in the loop that includes residues G259 to H278. An additional calculation of the electrostatic potential for the α/β-barrel domain without the loop G259–H278, shows an enhancement of the positive patch at the C-terminal of the α/β-barrel. Under these conditions, the electrostatic properties resemble much more the ones corresponding to the other enzymes described above. The values of the electrostatic flux due to the backbone and the α/β-barrel are 1.7 kTÅ/e and 3.3 kTÅ/e, respectively (Table 1). Since the loop G259–H278 is positioned right at the C-terminal end of the α/β-barrel domain, our calculations suggest that the conformation of this loop is stabilized by electrostatic interactions, i.e., the acidic residues D260, E263, E266, and D267 are embedded in the region of positive electrostatic potential generated by the rest of the α/β-barrel domain, giving rise to a favorable interaction. These calculations suggest that the residues in the loop G259–H278 could play a critical role in binding the positively charged substrate. In order to assess the conservation of the amino acid residues in this loop, we searched the Swissprot database of sequences but unfortunately found only one sequence corresponding to TMADH. On the other hand, experimental evidence seems to lend support to our hypothesis, given that W264, a residue in this loop, has been shown to be both involved in the binding of the substrate and a known inhibitor of TMADH. Hence, the generic electrostatic pattern of the α/β-barrel is also observed for this enzyme when the extra loop containing residues G259-H278 is removed.

Narbonin

NAR is a protein from the seeds of legumes with no known enzymatic activity. Interestingly, two recent publications propose that NAR could potentially be related to glycosyl hydrolases (Coulson, 1994; Sakon et al., 1996). The net charge of NAR is $-12.0e$ which might lead one to believe that this protein would favor the binding of a positively charged substrate. Our calculation, based on a high-resolution crystal structure, 1.8Å (Hennig et al., 1992), helps clarify this issue. We observe that despite its large negative charge, NAR exhibits an electrostatic field that could potentially

guide a negatively charged compound into its putative active site. Cursory inspection of NAR's solvent-accessible surface shows a large cavity at the C-terminal end of the β-strands, defined by the side chains of residues Y8, R87, H130, E132, S167, N170, Q191, N194, W261, F259, and by the backbone of P166. This could be the binding crevice for a putative substrate.

Conclusions

We have shown that the α/β-barrel backbone has a characteristic electrostatic pattern, and when measured in terms of the electrostatic flux it contributes substantially to the overall electrostatic properties of the α/β-barrel. The side chains help tailor the electrostatic field to attract each specific substrate to the active site. The electrostatic calculations carried out in the present work contribute to an understanding of the marked preference of α/β-barrel enzymes for negatively charged substrates. Furthermore, they show that using current models for treating electrostatic forces, the helices in an α/β-barrel do not contribute just locally near their own termini (Hol, 1978) but, rather, globally via all helices together, to the electrostatic properties of α/β-barrel enzymes.

Methods

Computation

Seven α/β-barrel enzymes, representing different evolutionary families, were chosen for analysis from the Protein Data Bank (Bernstein et al, 1977): fructose-1,6-bisphosphate aldolase (EC 4.1.2.13) (1fba)[6] (Malek et al., 1988; Hester et al., 1991), TMADH (EC 1.5.99.7) (2tmd) (Lim et al., 1988; Bellamy et al., 1989; Barber et al., 1992), pyruvate kinase (EC 2.7.1.40) (1pkn) (Larsen et al., 1994), mandelate racemase (EC 5.1.2.2) (2mnr) (Neidhart et al., 1990, 1991), TIM (EC 5.3.1.1.) (1tim) (Banner et al., 1975; Alber et al., 1981), glycolate oxidase (EC 1.1.3.15) (1gyl) (Lindqvist, 1989; Lindqvist & Branden, 1989; Macheroux et al., 1993), and narbonin[7] (1nar) (Hennig et al., 1992). For TMADH, a multidomain enzyme, we only used a single domain which includes residues 1–382. Furthermore, the co-factors Mn^{2+} (in pyruvate kinase and in mandelate racemase), K^+ (in mandelate racemase), and the prosthetic group FMN (in glycolate oxidase and in TMADH) were included in our electrostatic calculations, whereas pyruvic acid, PYR (in pyruvate kinase) and adenosine diphosphate, ADP (in TMADH), were not included.

Structural superpositions were performed based on main-chain C_α atoms, using the program HOMOLOGCORE (P. A. Karplus), which employs the overlay strategy developed by Chothia and Lesk (1986). The equivalent secondary structural elements which seed the algorithm were chosen manually and included only residues from the eight β-strands. Residues were identified as equivalent based on a 5.0 Å cutoff.

The program DelPhi was used to obtain a numerical solution of the Poisson-Boltzmann equation. This procedure treats the protein and the solvent as two different homogeneous dielectric media, embedded in a cubic grid (Klapper et al., 1986; Honig & Nicholls, 1995). The protein is represented by a cavity of low dielectric constant ($\epsilon = 4$), and the surrounding solvent is represented by a dielectric constant with $\epsilon = 78.3$, containing counterions, which correspond to an ionic strength of 0.050 M. The boundary between the protein and the solvent is calculated as the solvent-accessible surface of the molecule (Connolly, 1983a, 1983b). A set of partial charges that correspond to the "united-atom" representation of the amino acid residues (Weiner & Kollman, 1981; Singh et al., 1986) were assigned to the non-hydrogen atoms and to the polar hydrogen atoms. Titratable residues aspartic acid, glutamic acid, lysine, and arginine were assumed to be charged, whereas histidine, cysteine, and tyrosine were considered to be neutral. It should be noted that the assignment of partial charges to the atoms of all the residues, implies that the models take into consideration the permanent dipole moments associated with the backbone and polar (neutral) side chains. The polar hydrogen atoms were added to each structure using the program SYBYL (Tripos, St. Louis). Partial charges for the co-factor FMN were computed using the program MOPAC (Stewart, 1993). A single DelPhi calculation using a nonlinear approximation of the Poisson-Boltzmann equation and the protein filling 50% of the cubic grid was enough to produce electrostatic potential maps[8] of the α/β-barrels.

Electrostatic flux

The electrostatic flux, $\mathcal{F}$, through a surface $\vec{A}$ is calculated according to the following equation:

$$\mathcal{F} = \int_A \vec{E}\cdot d\vec{A} \approx \sum_{i=1}^{n} \vec{E}i\cdot d\vec{A}i = \frac{\vec{A}}{n}\cdot\sum_{i=1}^{n}\vec{E}i = \vec{A}\cdot\langle\vec{E}\rangle$$

where $\vec{A}$ is a vector whose magnitude is the area of the square surface selected near the active site and its direction is perpendicular to the square ($\vec{A}$ was chosen so that it points towards the active-site region in all the cases). The integration over the surface is approximated by a summation; the surface is partitioned into n equal square elements of area $d\vec{A}i$, and $\vec{E}i$, the local electrostatic field, is evaluated on each area element; $\langle\vec{E}\rangle$ indicates the mean electrostatic field over the surface.

The mean electrostatic flux was computed on a 5 Å × 5 Å box positioned in front of the C-terminal end of the β-strands and outside the protein surface, as shown in Figure 2. The placement of the box was chosen to be relevant for substrate binding. This task was carried out manually using the commercial software InsightII (MSI). In each case the closest distance of any grid point to any atom in the enzyme was greater than 5.0 Å. The size of the square box was selected to avoid large variations of the electrostatic field within it, and at the same time allow a sufficient sampling of the electrostatic flux. The square box was subdivided into grid points separated by 0.5 Å and the coordinates of these points were given as input to the DelPhi calculations. The DelPhi program retrieved the values of the electrostatic potential and field at those positions. The electrostatic flux was then computed using the expression given above, where the average electrostatic field was computed over all the grid points of the square box. In order to provide some estimation of the errors incurred in the calculations of the flux, two types of cubic grid were used for the DelPhi calculations, one with 65^3 grid-points and the second with 129^3 grid-points. The values resulted from these calculations differ by less than 10%.

[6] Brookhaven Protein Data Bank entry code for the coordinate set.

[7] Although narbonin does not have any known enzymatic function, it is referred to as an enzyme throughout the text to simplify matters.

[8] Potential maps and PDB files of the enzymes with the exact orientation used in the calculations are available at the following anonymous ftp site: ftp.tc.cornell.edu, directory pub/ripoll/BARRELS.

Visualization tools

Visualization of the electrostatic potential data obtained from DelPhi, the molecular structure, and the solvent accessible surface was performed using the programs GRASP (Nicholls et al., 1991) and Data Explorer™ (DX) (IBM) in conjunction with a set of chemistry modules (Gillilan & Ripoll, 1995), and InsightII (MSI). The two-dimensional electrostatic field lines were obtained by computing the numerical gradient of the potential values on the plane. Points within a circle lying on this plane were used to initiate the streamlines. We varied the position of the intersecting plane to maximize the visualization of the electric field lines and the electrostatic isopotential projected onto this plane. The vectors normal to the planes studied here (data not shown) are perpendicular to the α/β-barrel axis.

Acknowledgments

We thank the reviewers of the manuscript for their interesting remarks. This research project was conducted as part of the Cornell Theory Center's 1995 Supercomputing Program for Undergraduate Research (SPUR), which is funded by the National Science Foundation's Research Experiences for Undergraduates program. The activities of the Theory Center are supported by major funding from the National Science Foundation and New York State, with additional funding from the National Center for Research Resources at NIH, the Advanced Research Projects Agency, IBM, and other members of the Cornell Theory Center's Corporate Research Institute. We thank R. E. Gillilan (CTC) for access to the chemistry modules for the DX program. This research was supported by a grant from the National Institutes of Health (P41RR-04293). We thank Drs. Barry Honig and Anthony Nicholls for providing us with the programs DelPhi and GRASP. We thank the National Institutes of Health for financial assistance in the form of a Program Project Grant, NIH GM 44874.

References

Alber T, Banner DW, Bloomer AC, Petsko GA, Phillips D, Rivers PS, Wilson IA. 1981. On the three-dimensional structure and catalytic mechanism of triose phosphate isomerase. *Phil Trans R Soc Lond B 293*:159–171.

Antosiewicz J, McCammon JA, Wlodek ST, Gilson MK. 1995. Simulation of charge-mutant acetylcholinesterases. *Biochemistry 34*:4211–4219.

Baldwin TO, Christopher JA, Raushel FM, Sinclair JF, Ziegler MM, Fisher AJ, Rayment I. 1995. Structure of bacterial luciferase. *Curr Op Struct Biol 5*:798–809.

Banner DW, Bloomer AC, Petsko GA, Phillips DC, Pogson CI, Wilson IA, Corran PH, Furth AJ, Milman JD, Offord RE, Priddle JD, Waley SG. 1975. Structure of chicken muscle triose phosphate isomerase determined crystallographically at 2.5 Å resolution using amino acid sequence data. *Nature 255*:609–614.

Barber MJ, Neame PJ, Lim LW, White S, Mathews FS. 1992. Correlation of X-ray deduced and experimental amino acid sequences of trimethylamine dehydrogenase. *J Biol Chem 267*:6611–6619.

Bellamy HD, Lim LW, Mathews FS, Dunham WR. 1989. Studies of crystalline trimethylamine dehydrogenase in three oxidation states and in the presence of substrate and inhibitor. *J Biol Chem 264*:11887–11892.

Bernstein FC, Koetzle TF, Williams GJB, Meyer EF Jr, Brice MD, Rodgers JR, Kennard O, Shimanouchi T, Tasumi M. 1977. The Protein Data Bank: A computer-based archival file for macromolecular structures. *J Mol Biol 112*:535–542.

Bränden CI. 1980. Relations between structure and function of α/β-proteins. *Quarter Rev Biophys 13*:317–338.

Chothia C, Lesk A. 1986. The relation between the divergence of sequence and structure in proteins. *EMBO J 5*:823–826.

Connolly ML. 1983a. Solvent-accessible surfaces of proteins and nucleic acids. *Science 221*:709–713.

Connolly ML. 1983b. Analytical molecular surface calculation. *J Appl Crystallogr 16*:548–558.

Coulson AFW. 1994. A proposed structure for "family 18" chitinases. A possible function for narbonin. *Febs Lett 354*:41–44.

Farber GK. 1993. An α/β barrel full of evolutionary trouble. *Curr Op Struct Biol 3*:409–412.

Farber GK, Petsko GA. 1990. The evolution of α/β-barrel enzymes. *Trends Biochem Sci 15*:228–234.

Getzoff ED, Cabelli DE, Fisher CL, Parge HE, Viezzoli MS, Banci L, Hallewell RA. 1992. Faster superoxide dismutase mutants designed by enhancing electrostatic guidance. *Nature 358*:347–351.

Gillilan R, Ripoll DR. 1995. Visualizing enzyme electrostatics with IBM Visualization Data Explorer. In: Bowie J, ed. *Data Visualization in Molecular Science*. Greenwich, Connecticut: Manning Publications Co. and Addison-Wesley Publishing Company, Inc. pp 61–81.

Gilson MK, Straatsma TP, McCammon JA, Ripoll DR, Faerman CH, Axelsen PH, Silman I, Sussman JL. 1994. Open "back door" in a molecular dynamics simulation of acetylcholinesterase. *Science 263*:1276–1278.

Hennig M, Schlesier B., Dauter Z, Pfeffer S, Betzel C, Höhne WE, Wilson KS. 1992. A TIM barrel protein without enzymatic activity? Crystal structure of narbonin at 1.8 Å resolution. *FEBS Lett 306*:80–84.

Hester G, Brenner-Holzach O, Rossi FA, Struck-Donatz M, Winterhalter KH, Smit JDG, Piontek K. 1991. The crystal structure of fructose-1,6-bisphospate aldolase from *Drosophila melanogaster* at 2.5 Å resolution. *FEBS Lett 292*:237–242.

Hol WGJ, van Duijnen PT, Berendsen HJC. 1978. The α-helix dipole and the properties of proteins. *Nature 273*:443–446.

Honig B, Nicholls A. 1995. Classical electrostatics in biology and chemistry. *Science 268*:1144–1149.

Klapper I, Hagstrom R, Fine RM, Sharp KA, Gilson MK, Honig B. 1986. Focusing of electric fields in the active site of Cu–Zn superoxide dismutase: Effects of ionic strength and amino acid modification. *Proteins: Struct Funct Genet 1*:47–59.

Kraulis PJ. MOLSCRIPT: A program to produce both detailed and schematic plots of protein structures. 1991. *J Appl Cryst 24*:946–950.

Larsen TM, Laughlin LT, Holden HM, Rayment I, Reed GH. 1994. Structure of rabbit muscle pyruvate kinase complexed with Mn^{2+}, K^+, and pyruvate. *Biochemistry 33*:6301–6309.

Lim LW, Mathews FS, Steenkamp DJ. 1988. Identification of ADP in the iron–sulfur flavoprotein trimethylamine dehydrogenase. *J Biol Chem 263*: 3075–3078.

Lim LW, Shamala N, Mathews FS, Steenkamp DJ, Hamlin R, Xuong NH. 1986. Three-dimensional structure of the iron–sulfur flavoprotein trimethylamine dehydrogenase at 2.4 Å resolution. *J Biol Chem 261*:15140–15146.

Lindqvist Y. 1989. Refined structure of spinach glycolate oxidase at 2 Å resolution. *J Mol Biol 209*:151–166.

Lindqvist Y, Bränden C I. 1989. The active site of spinach glycolate oxidase. *J Biol Chem 264*:3624–3628.

Luty BA, Wade RC, Madura JD, Davis ME, Briggs JM, McCammon JA. 1993. Brownian dynamics simulations of diffusional encounters between triose phosphate isomerase and glyceraldehyde phosphate: electrostatic steering of glyceraldehyde phosphate. *J Phys Chem 97*:233–237.

Macheroux P, Kieweg V, Massey V, Soderlind E, Stenberg K, Lindqvist Y. 1993. Role of tyrosine 129 in the active site of spinach glycolate oxidase. *Eur J Biochem 213*:1047–1054.

Malek AA, Hy M, Honegger A, Rose K, Brenner-Holzach O. 1988. Fructose-1,6-bisphosphate aldolase from *Drosophila melanogaster* primary structure analysis, secondary structure prediction, and comparison with vertebrate aldolases. *Arch Biochem Biophys 266*:10–31.

Nakamura H. 1996. Roles of electrostatic interactions in proteins. *Quarter Rev Biophys 29*:1–90.

Neidhart DJ, Howell PL, Petsko GA, Powers VM, Li R, Kenyon GL, Gerlt J A. 1991. Mechanism of the reaction catalyzed by mandelate racemase. 2. Crystal structure of mandelate racemase at 2.5 Å resolution: Identification of the active site and possible catalytic residues. *Biochemistry 30*:9264–9273.

Neidhart DJ, Kenyon GL, Gerlt JA, Petsko GA. 1990. Mandelate racemase and muconoate lactonizing enzyme are mechanistically distinct and structurally homologous. *Nature 347*:692–694.

Nicholls A, Sharp KA, Honig B. 1991. Protein folding and association: Insights from the interfacial and thermodynamic properties of hydrocarbons. *Proteins: Struct Funct Genet 11*:281–296.

Orengo CA, Jones DT, Thornton JM. 1994. Protein superfamilies and domain superfolds. *Nature 372*:631–634.

Reardon D, Farber GK. 1995. The structure and evolution of α/β barrel proteins. *FASEB J 9*: 497-503.

Ripoll DR, Faerman CH, Axelsen PH, Silman I, Sussman JL. 1993. An electrostatic mechanism for substrate guidance down the aromatic gorge of acetylcholinesterase. *Proc Natl Acad Sci USA 90*:5128–5132.

Ripoll DR, Faerman CH, Gillilan R, Silman I, Sussman JL. 1995. Electrostatic properties of human acetylcholinesterase. In: Quinn DM, Balasubramanian AS, Doctor BP, Taylor P, eds. *Enzymes of the Cholinesterase Family*. New York: Plenum Press. pp 67–70.

Sakon J, Adney WS, Himmel ME, Thomas SR, Karplus PA. 1996. Crystal structure of thermostable family 5 endocellulase E1 from *Acidothermus cellulolyticus* in complex with cellotetraose. *Biochemistry 35*:10648–10660.

Schreiber G, Fersht AR. 1996. Rapid, electrostatically assisted association of proteins. *Nat Struct Biol 3*:427–431.

Shafferman A, Ordentlich A, Barak D, Kronman C, Ber R, Bino T, Ariel N, Osman R, Velan B. 1994. Electrostatic attraction by surface charge does not contribute to the catalytic efficiency of acetylcholinesterase. *EMBO J 13*:3448–3455.

Singh UC, Weiner PK, Caldwell J, Kollman PA. 1986. *AMBER 3.0*. San Francisco: University of California.

Spassov VZ, Karshikoff AD, Ladenstein R. 1994. Optimization of the electrostatic interactions in proteins of different functional and folding type. *Protein Sci 3*:1556–1569.

Stewart JJP. 1993. *MOPAC 93 Manual*. Tokyo: Fujitsu Ltd.

Weiner PK, Kollman PA. 1981. AMBER. Assisted model building with energy refinement. A general program for modeling molecules and their interactions. *J Comp Chem 2*:287–303.